Neuropharmacology 292 (2026) 110944

Contents lists available at ScienceDirect

Neuropharmacology

journal homepage: www.elsevier.com/locate/neuropharm

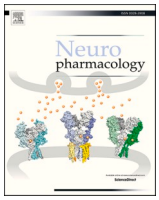

Protective effects of adenosine A2B receptor antagonism in a cuprizone-induced demyelination model

Federica Cherchi [a,b,1], Martina Venturini [a,1], Lucia Frulloni [a], Federica Panozzi [a], Giada Magni [c], Clara Santalmasi [a], Camilla Maestrelli [d], Maria Grazia Giovannini [d], Elisabetta Coppi [a], Daniele Lana [d,*,1], Anna Maria Pugliese [a,1]

[a] Department of Neuroscience, Psychology, Drug Research and Child Health (NEUROFARBA), University of Florence, Florence, Italy
[b] Department of Neuroscience and Human Genetics, Meyer Children's Hospital IRCCS, Florence, Italy
[c] Istituto di Fisica Applicata "Nello Carrara", Consiglio Nazionale Delle Ricerche (CNR-IFAC), Sesto Fiorentino, Italy
[d] Section of Clinical Pharmacology and Oncology, Department of Health Sciences, University of Florence, Florence, Italy

ARTICLE INFO

Keywords:
Purinergic signalling
Demyelinating diseases
Oligodendrogliogenesis
Myelin repair
Astrogliosis
Microgliosis

ABSTRACT

Demyelinating diseases are characterized by the progressive loss of myelin in the central nervous system (CNS). Myelin protection can be achieved by fostering the differentiation of oligodendrocyte progenitor cells to mature oligodendrocytes, the only myelinating cells in the brain. Oligodendrocytes maturation is sustained, among others, by the neuromodulator adenosine through the activation of its specific receptors: A_1, A_{2A}, A_{2B}, A_3, all expressed in the brain on neurons and glial cells. The role of A_{2B} receptors (A2BRs) in a cuprizone-induced demyelination model in male C57BL/6 mice was investigated by administering the selective A2BR agonist BAY60-6583 or antagonist PSB 603 during the last 2 weeks of a 5-week cuprizone-based diet. We performed body weight evaluation, behavioural tests and immunofluorescence analysis. Cuprizone-fed mice showed a significant decrease in body weight gain, a motor impairment and a reduced spontaneous mobility. These effects were associated with a decrease in myelin levels, a reactive astrogliosis and microgliosis in corpus callosum medialis, striatum and motor cortex. PSB 603, was able to prevent cuprizone effects on glia, whereas both compounds promoted a significant recovery in motor deficits. The antagonism of A2BRs might represent an attractive strategy to alleviate myelin damage and glial activation in the CNS under conditions of demyelination.

1. Introduction

Demyelinating disorders of the central nervous system (CNS), such as multiple sclerosis (MS), are characterized by the loss of myelin sheaths, leading to impaired neuronal conduction and neurological deficits. These diseases involve complex pathological mechanisms including oxidative stress, mitochondrial dysfunction, and chronic inflammation, in which glial cells play a central role. The cuprizone (CPZ) model represents a well-established paradigm of non-immune-mediated demyelination, characterized by selective oligodendrocyte (OL) loss, reactive astrogliosis, microglial activation, and subsequent remyelination upon toxin withdrawal (Vega-Riquer et al., 2019).

Among the neuromodulator systems involved in CNS injury, adenosine signaling plays a pivotal role through its four G-protein-coupled receptors (A_1, A_2A, A_2B, A_3), in modulating different processes such as the excitability of neurons and synaptic transmission, and in regulating neuroinflammation and glial reactivity (Fredholm et al., 2011). Additionally, adenosine signalling is critical in hypoxic or ischaemic conditions, in which adenosine levels increase in response to metabolic alteration or tissue injury. This elevation in extracellular adenosine is a key factor in the progression of the above pathological conditions (Pedata et al., 2016). In demyelinating diseases the involvement of purinergic signalling is well established (see Coppi et al., 2021). Nevertheless, to date an increase in adenosine extracellular concentration in these conditions can only be hypothesized.

Among all adenosine receptors, the adenosine A_{2B} receptor (A2BR) is of particular interest due to its low affinity for the neuromodulator and its upregulation under pathological conditions related to elevated extracellular adenosine levels (Coppi et al., 2020; Wei et al., 2013). It is known that A2BRs are expressed in astrocytes, microglia, and

* Corresponding author.
E-mail address: daniele.lana@unifi.it (D. Lana).
[1] these authors equally contributed to the paper.

https://doi.org/10.1016/j.neuropharm.2026.110944
Received 8 January 2026; Received in revised form 20 March 2026; Accepted 21 March 2026
Available online 24 March 2026

oligodendrocytes, where they modulate the release of inflammatory mediators and influence glial reactivity. In particular, it is demonstrated that A2BR activation inhibits oligodendrocyte progenitor cell (OPC) differentiation and myelin gene expression, partly by suppressing K^+ currents and modulating the sphingosine-1-phosphate signaling axis (Cherchi et al., 2021a; Coppi et al., 2020). Accordingly, silencing of A2BR has been shown to promote OPC maturation in vitro whereas selective pharmacological blockade exerts neuroprotective effects in models of oxygen-glucose deprivation (Coppi et al., 2020; Fusco et al., 2018).

Notably, Wei and collaborators (Wei et al., 2013), investigating the role of A_2BR in experimental autoimmune encephalomyelitis (EAE), observed that pharmacological blockade with selective antagonists such as CVT-6883 or MRS1754 alleviates clinical symptoms and protects the CNS from immune-mediated damage. Consistently, A2BR knockout ($A2BR^{-/-}$) mice develop a markedly milder EAE phenotype (Wei et al., 2013).

Despite these findings, the role of A2BRs in toxin-induced demyelination remains unexplored. In this context, to investigate the effect of A2BR modulation during demyelination, we used the CPZ model in C57BL/6 mice, a well-established non-autoimmune model that induces reversible demyelination through oligodendrocyte toxicity. This model allows for the evaluation of both the demyelination or remyelination phases and potential therapeutic interventions without the confounding effects of peripheral immune cell infiltration. In our study, we tested both an A2BR agonist (BAY60-6583) and a selective antagonist (PSB 603) during CPZ administration. This study aimed to clarify the role of A2BR signaling during demyelination, and to evaluate whether pharmacological interference of this receptor could promote myelin protection and/or glial regulation in a context-dependent manner.

2. Materials and methods

2.1. Animals

All animal procedures were conducted according to the Italian Guidelines for Animal Care, DL 116 / 92, application of the European Communities Council Directive (86 / 609 /EEC) and approved by the Committee for Animal Care and Experimental Use of the University of Florence. Male C57BL/6 mice were obtained from Charles River Laboratories, Italy. The approved animal protocol number is 936/2021-PR. Animals were allowed to acclimate for about 4 days, to adjust to their new environment, before the study began. Mice were maintained under a normal day-night cycle (12/12 h) with constant temperature and humidity control throughout the entire period, with access to food and water *ad libitum*. Basic cage enrichments, including nesting material (crinkle nest), pipe tubes (polyvinyl chloride), and red shelters to reduce stress were provided.

2.2. Cuprizone model

To induce oligodendrocyte degeneration and demyelination, 42-48 days old male C57BL/6 mice were fed a diet containing 0.2% Bis (cyclohexanone)oxaldihydrazone (Cuprizone, CPZ, Sigma-Aldrich). Standard laboratory mouse chow (7g chow per mouse/day), provided by the animal facility, was ground to a powder to ensure uniform amalgamation of the CPZ. All mice were acclimatized with powdered control diet for 4 days prior to the start of the experiments. Control mice received the same powdered diet without CPZ for the entire duration of the study.

The protocol consisted of a period during which animals were exposed to CPZ for 5 consecutive weeks (Fig. 1). At the end of the third week, the animals were divided into different experimental groups and treated for the last two weeks with A2BR ligands by intraperitoneal injection.

2.3. Drug administration and experimental groups

Adenosine A2BR antagonist 8-(4-(4-(4-Chlorophenyl) piperazide-1-sulfonyl) phenyl)-1-propylxanthine (PSB 603) (Merck, Germany) was dissolved in dimethyl sulfoxide (DMSO) 0.1% in saline and was administered at the dose of 0.05 mg/kg, based on literature (Tanaka et al., 2020). Adenosine A2BR agonist 2-[[6-amino-3,5-dicyano-4-[4-(-cyclopropylmethoxy)phenyl]-2-pyridinyl]thio]-acetamide (BAY60-6583) (Tocris, United Kingdom) was dissolved in DMSO 0.1% in saline and was administered at 0.1 mg/kg, a dose previously shown to selectively activate A2BR *in vivo* (Dettori et al., 2021), consistent with its EC50 extrapolated by in vitro and *in vivo* experiments (Coppi et al., 2020). Moreover, a dose of 0.1 mg/kg has been shown to be effective in protecting against peripheral arterial lesions (Bot et al., 2012) and lung injury induced by mechanical ventilation in mice (Eckle et al., 2008).

As a vehicle, normal saline containing 0.1% DMSO was used, corresponding to the highest DMSO concentration administered in drug-treated groups. All compounds were administered intraperitoneally (i.p.) once every 2 days for 2 weeks during the final phase of CPZ intoxication, i.e., from week 3 to week 5.

Mice were randomly assigned to experimental groups. Specifically.

- Control (CTR): standard diet + vehicle (n = 6);
- CPZ: CPZ-enriched diet + vehicle (n = 6);
- PSB: CPZ-enriched diet + PSB 603 (0.05 mg/kg, n = 5);
- BAY: CPZ-enriched diet + BAY60-6583 (0.1 mg/kg, n = 4).

All treatments were performed blind as to experimental conditions. At the end of the CPZ intake corresponding to two days after the last drug injection, behavioural tests were performed, and animals were sacrificed for immunohistochemical analysis.

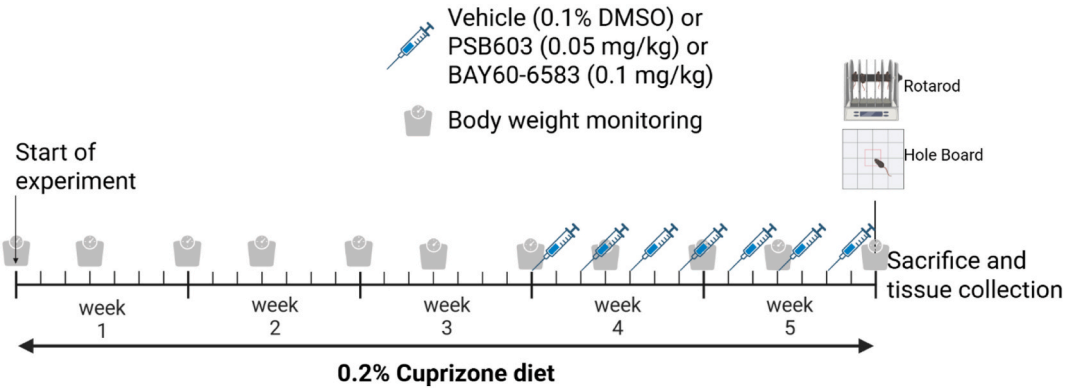

Fig. 1. Timeline of the study and experimental design (Created with https://biorender.com).

2.4. Body weight evaluation

Mice used in the present research weighed between 20 and 25 g at the beginning of the experiment. Body weight was monitored twice a week throughout the study. Changes in body weight were evaluated for each animal relative to its baseline weight, recorded before the start of the experimental procedures.

2.5. Rotarod test

Animal balance and motor coordination were tested using a rotating metal rod. Before experiment, mice were acclimated on the rotarod via 1 training session, lasting 3 min, performed the day before the experiment. Animals were tested at the end of the fifth week to evaluate the effect of CPZ in comparison to control animals. The apparatus consisted of a base platform, a rotating rod, and a non-slippery surface. The rod, 30 cm in length and 3 cm in diameter, was divided into 5 equal sections by 6 disks (Galeotti et al., 2013). Each animal was individually tested for 3 min on the apparatus, with the rod-rotating speed of 31 rpm. The latency to the first fall was recorded, applying a minimum of 10-s cut-off, to minimize potential bias related to operator handling.

2.6. Hole-board test

The Hole-board test is mainly used for assessing exploratory and social behaviours in rodents. The animal is placed in an arena with regularly arranged holes on the floor (Takeda et al., 1998). Both frequency and duration of spontaneous elicited hole-poking behaviour were measured. The Hole-board test apparatus (Hole-board Device, Ugo Basile, Varese, Italy) consisted of a square elevated arena (40 cm × 40 cm; 1 m above the floor), featuring 16 evenly spaced, flush-mounted cylindrical holes, each with a diameter of 3 cm, arranged in a 4x4 equidistant grid pattern. Each mouse was individually placed on the left side of the board and allowed to freely explore it for a duration of 5 min. Two infrared sensors, positioned across the midpoints of opposite sides of the platform, divided the surface into 4 equal quadrants and automatically detected the movement of the animal, recording its locomotor activity. Miniature photoelectric sensors installed in each of the 16 holes detected and recorded the exploratory behaviour of the mice as they investigated the holes. Each mouse was individually tested for spontaneous mobility (number of quadrants exchanged during the time of recording) and anxiety-like behaviour (number of head dips in the holes of the board). We also evaluated the time spent in the center of the board as indicative either of avoidance of the perimeter of the elevated arena (source of fear for the mouse) or reduced mobility.

2.7. Immunohistochemistry

Two days after the last CPZ injection, mice were anesthetized with Zoletil ® 50/50 (Tiletamine hydrochloride/Zolazepam hydrochloride; 45 mg/kg i.p., Virbac, Carros, Francia) and were perfused transcardially with an ice-cold 4% paraformaldehyde in PBS. Brains were post-fixed overnight and cryoprotected in a 18% sucrose solution in PBS for at least 48 h (Dettori et al., 2021). Brains were then frozen in 5-methylbutane chilled on dry ice and stored at −80 °C until their processing. Mice brains were frozen in Optimal Cutting Temperature (O.C.T.) (Kaltek, Italy), and 30 μm-thick coronal sections were cut with a cryostat at +0.98 mm from Bregma according to the mouse brain atlas. The corpus callosum was used as an anatomical landmark to infer the location of the slice in relation to bregma. Brain sections were collected and stored at –20 °C in an antifreeze solution consisting of 30% glycerol, 30% ethylene glycol, 15.4 mM NaH_2PO_4*H_20, 38.4 mM Na_2HPO_4. Immunohistochemistry was performed with the free-floating method (Giovannini, 2002; Lana et al., 2014; Mercatelli et al., 2016).

2.7.1. Immunofluorescence labelling

Day 1: Sections were washed three times in a 24-wells multiwell plate with PBS-TX (0.3% Triton X-100 in PBS). Before incubation with primary antibodies, all sections were incubated for 60 min with Blocking Buffer (BB) containing 10% Normal Goat Serum (Product Code: S-1000, Vector, Burlingame, CA, USA) in PBS-TX. After BB, sections were incubated overnight at 4 °C under slight agitation in a solution with: i) mouse anti-Myelin Basic Protein (MBP) (1:400 in BB; Product Code: 83683S, Cell Signaling, Danvers, MA, USA), to immunostain oligodendrocytes (single labelling immunofluorescence), or ii) rabbit anti-Ionized Calcium Binding Adaptor 1 (IBA1) antibody (1:300 in BB; Product code: 016–20001 FUJIFILM Wako, Osaka, JP), to immunostain total microglia (double labelling immunofluorescence).

Day 2: Sections were washed three times in PBS-TX and then incubated for 2 h at room temperature in the dark with specific secondary antibodies: i) AlexaFluor 555 donkey anti-mouse (1:500 in BB; Product code: A31570, Thermo Fisher, Waltham, MA, USA) (single labelling immunofluorescence) or ii) AlexaFluor 635 goat anti-rabbit secondary antibody (1:400 in BB; Product code: A31577, Thermo Fisher) (double labelling immunofluorescence). Only in case of double labelling, sections were washed in PBS-TX and further immunostained (2h of incubation at room temperature) using a mouse anti-Glial Fibrillary Acidic Protein (GFAP) antibody conjugated with the fluorochrome AlexaFluor 488 (1:500 in BB; Product code: MAB3402X, Millipore, Billerica, MA, United States). Finally after three washes in PBS-TX, slices were mounted on gelatin-coated slides with Vectashield mounting medium with DAPI to stain cell nuclei (Vectashield Product Code H-1200, Vector, Burlingame, CA, USA)., a.

2.8. Confocal microscopy and quantitative analysis

Immunohistochemical images were captured using a Leica SP8 laser scanning confocal microscope (Leica Microsystems, Mannheim, Germany), as described in Lana et al. (2024) and Sarti et al. (2025). Brain areas chosen (Regions of Interest, ROIs) for quantitative analysis were (i) corpus callosum medialis (CCM), motor cortex (CTX) (ii) and striatum (ST) (iii) (Fig. 2).

Quantitative analyses were performed using the software ImageJ (http://rsb.info.nih.gov/ij). MBP immunofluorescence was quantified by calculating the percentage of area fraction above a defined threshold within manually outlined ROIs (Khodanovich et al., 2019).

The density of astrocytes and microglia were expressed as cells/mm^2. Quantitative analyses of GFAP and IBA1 immunofluorescence were obtained from the percentage of GFAP positive or IBA1 positive pixels above a set threshold level using the threshold tool of ImageJ.

2.9. Statistical analysis

Data are presented as mean ± SEM (standard error of the mean). Statistical significance was evaluated by: Student's t-test, One-way ANOVA followed by appropriate post hoc test or Two-way ANOVA (repeated measures) followed by appropriate post hoc test. All statistical analyses were performed using GraphPad PRISM v.8 for Windows (GraphPad Software, San Diego, CA, USA). A probability value $P < 0.05$ was considered significant.

3. Results

3.1. Effect of A2BR ligands on CPZ–induced loss of body weight gain and locomotor activity

Male C57BL/6 mice at day 0 weighted 23-25 g. During the first three weeks of the CPZ-based diet, mice had a reduced body weight gain compared to the control group (Fig. 3A). Statistical analysis of body weight changes over time revealed a significant effect of both time ($F(6,133) = 9.487$, $P < 0.0001$) and treatment ($F(1,133) = 19.02$, $P <$

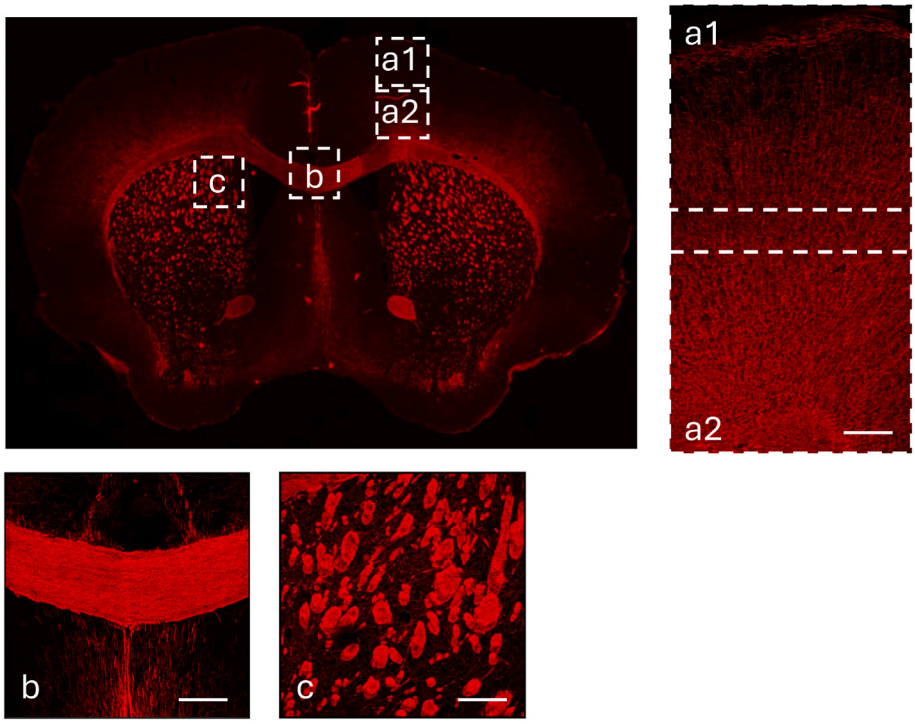

Fig. 2. Representative confocal images acquired from coronal brain sections showing the regions of interest (ROIs) selected for the immunohistochemical analyses. (a1-a2) motor cortex (CTX), (b) corpus callosum medialis (CCM), (c) striatum (ST).

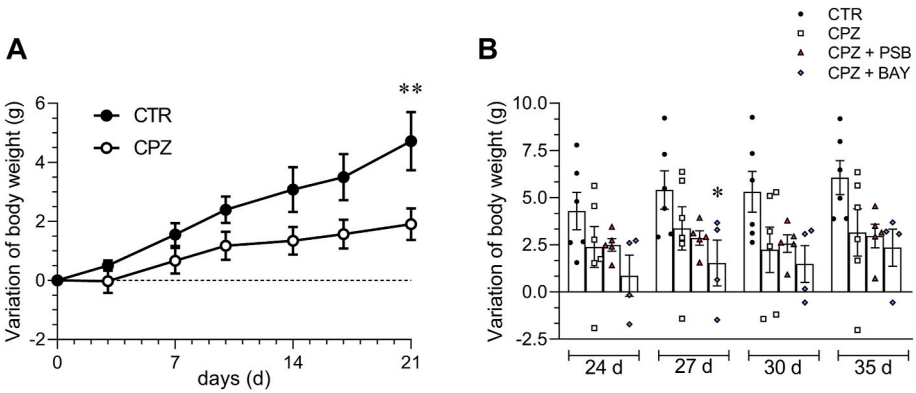

Fig. 3. Effects of CPZ diet and A2BR ligands administration on animal body weight. **A:** The graph illustrates changes in body weight (mean ± SEM) over time in control animals (CTR, n = 11) and CPZ-treated mice (CPZ, n = 11) during the first 3 weeks of CPZ treatment. **B:** Column bars show time-course of changes in body weight gain in control mice (CTR, n = 6) and CPZ-treated mice for the 2 last weeks of CPZ-feeding (CPZ, n = 5) in the presence of the adenosinergic ligands: PSB 603 (CPZ + PSB, n = 5) or BAY60-6583 (CPZ + BAY, n = 4). Data are expressed as mean ± SEM; *P < 0.05, **P < 0.01 vs CTR on the same day (Two-way ANOVA repeated measures followed by Bonferroni post hoc test (A) or One-way ANOVA followed by Dunnet post hoc test (B)).

0.0001), although no significant interaction between the two factors was observed (F(6,133) = 1.425, P = 0.2096). Specifically, while both groups showed a progressive increase in weight, Bonferroni's post hoc test revealed that the CPZ-treated group gained significantly less weight compared to the CTR group only at day 21 (t = 3.558, **P = 0.0036; Fig. 3A). The effects of different treatments (PSB 603 and BAY60-6583) on body weight were evaluated from day 24 to day 35 (Fig. 3B). One-way ANOVA did not show a significant overall effect of treatment at any of the time points analysed (day 24: F(3,17) = 2.068, P = 0.1424; day 27: F(3,17) = 2.459, P = 0.0979; day 30: F(3,17) = 2.736, P = 0.0757; day 35: F(3,17) = 2.813, P = 0.0706). Nevertheless, Dunnett's multiple comparisons test revealed a significant reduction in weight variation in the BAY-treated group compared to CTR at day 27 (q = 2.596, **P = 0.0493), while no significant differences were observed for the other treatment groups (CPZ and PSB 603) relative to CTR throughout the observation period. (Fig. 3B).

It is known that CPZ, causing demyelination in the CNS, leads to a range of behavioural alterations, including increased anxiety-like behaviour (Zhang et al., 2020). We used the Hole-board test to study spontaneous mobility (Fig. 4A), the exploratory activity (Fig. 4B) and the time spent in the center of the arena (Fig. 4C) of mice from the four experimental groups. In CPZ-fed animals we found a significant reduction of spontaneous mobility (Fig. 4A) and a significant increase of time spent in the centre of the board (Fig. 4C). One-way ANOVA revealed a significant effect of treatment (F(3,17) = 6.539, P = 0.0039) in spontaneous mobility. The Newman-Keuls post hoc test showed a significant reduction in the number of quadrant crossings in the CPZ group compared to CTR (q = 5.738, **P < 0.01). This behavioural impairment was effectively prevented by the administration of both PSB 603 (q = 4.695, #P < 0.05 vs CPZ) and BAY 60-6583 (q = 4.104, ##P < 0.01 vs

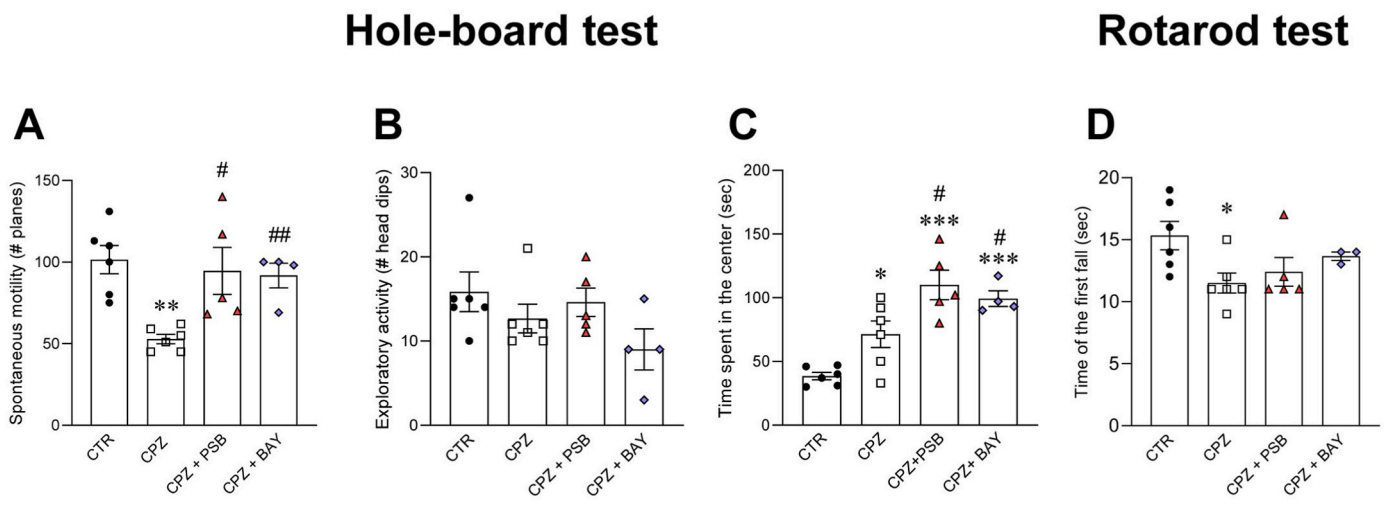

Fig. 4. Motor performance quantified using the Hole-board test and rotarod paradigm. **A-C**: Evaluation of spontaneous mobility, exploratory activity, and time spent in the center of the arena assessed by the Hole-board test. **A:** Animal spontaneous mobility is reduced in CPZ-treated mice, an effect reverted either by PSB 603 or BAY60-6583. **B:** Exploratory activity was not significantly different in all the groups. **C:** . CPZ increased the time spent in the center of the arena and this effect was significantly modulated by both A2BR ligands. **D:** The graph shows the time to first fall in the rotarod test in different experimental groups. CPZ intake significantly decreased this parameter and this effect was not modified either by PSB 603 or BAY60-6583. In all graphs data are expressed as mean ± SEM; *P < 0.05, **P < 0.01, ***P < 0.001 vs CTR; #P < 0.05, ##P < 0.01 vs CPZ (one-way ANOVA followed by Newman-Keuls (Fig. 4A–C) or Dunnett post hoc test (Fig. 4D). CTR, n = 6; CPZ, n = 6; CPZ + PSB, n = 5; CPZ + BAY, n = 3-4.

CPZ). Notably, no significant differences were observed between the CTR group and either the CPZ + PSB or CPZ + BAY groups, indicating a full recovery of the exploratory activity (Fig. 4A).

One-way ANOVA revealed a highly significant effect of treatment ($F(3,17) = 14.07$, $P < 0.0001$) also in the time spent in the centre of the board. The Newman-Keuls post hoc test showed that CPZ-treated mice spent significantly more time in the center compared to CTR animals ($q = 4.067$, *P < 0.05). This effect was further amplified in mice receiving the treatments, as both the CPZ + PSB group ($q = 8.445$, ***P < 0.0001) and the CPZ + BAY group ($q = 6.731$, ***P < 0.001) showed a marked increase in time spent in the center relative to the CTR group. Furthermore, both PSB 603 and BAY60-6583 treatments significantly increased the time spent in the center even when compared to the CPZ-only group ($q = 4.567$, #P < 0.05 and $q = 3.093$, #P < 0.05, respectively; Fig. 4C).

However, no effect of CPZ was found on exploratory activity as measured by hole-board head dips (Fig. 4B). One-way ANOVA revealed no significant differences among the experimental groups ($F(3,17) = 1.823$, $P = 0.1813$). Consequently, the Newman-Keuls post hoc test did not identify any significant comparisons between groups, suggesting that this specific exploratory parameter was not significantly altered by CPZ administration or by the subsequent pharmacological treatments.

Moreover, CPZ has been reported to impair both motor coordination and balance (Vega-Riquer et al., 2019; Zirngibl et al., 2022). To assess these effects, we utilized the rotarod test (Fig. 4D). As expected, after 5 weeks of CPZ diet, which is the time at which demyelination is at its peak, animals treated with the toxin tended to fell from the rod significantly earlier than the control group (Fig. 4D). Pharmacological treatment with either BAY60-6583 or PSB 603 did not result in any significant improvement in this behavioural parameter. One-way ANOVA showed a trend toward an effect of treatment, although it did not reach full statistical significance ($F(3,16) = 2.983$, $P = 0.0624$). Nevertheless, Dunnett's post hoc test revealed that CPZ-treated mice had a significantly shorter latency to the first fall compared to the CTR group ($q = 2.852$, *P = 0.0309). In contrast, no significant differences were observed between CTR animals and those treated with either PSB 603 ($q = 2.081$, $P = 0.1347$) or BAY60-6583 ($q = 1.013$, $P = 0.6412$).

3.2. Effect of A2BR ligands on CPZ–induced loss of myelin basic protein expression in the corpus callosum medialis, motor cortex and striatum

As previously described, MBP is one of the key proteins associated to myelin sheath deposition (Kornguth and Anderson, 1965; Laatsch et al., 1962) and can be used to assess demyelination processes. Thus, to quantify myelin damage induced by CPZ, we performed immunohistochemical analysis to determine MBP expression in the different ROIs under investigation. In Fig. 5A we report representative confocal images of MBP-immunostaining in the three ROIs, from the qualitative images shown in Fig. 5A, it appears that CPZ significantly decreased MBP immunofluorescence in all the brain areas investigated, confirming significant demyelination in the regions examined. This effect was reverted after treatment with PSB 603 (Fig. 5A). The selective stimulation of A2BR with BAY60-6583 induced a further decrease in MBP immunostaining. As indicated in Fig. 5B–D, quantitative analyses revealed that PSB 603 treatment resulted in a significant recovery of the damage, rescuing MBP expression levels to control values. On the contrary, BAY60-6583 exacerbated the damage in CCM (Fig. 5B) and CTX (Fig. 5C) and did not modify CPZ effect in ST (Fig. 5D).

In the corpus callosum, One-way ANOVA revealed a highly significant effect of treatment ($F(3,17) = 29.59$, $P < 0.0001$). Newman-Keuls post hoc test showed a drastic reduction of MBP area in CPZ-treated mice compared to CTR ($q = 8.932$, ***P < 0.0001). Treatment with PSB effectively prevented this loss, restoring MBP levels to values comparable to CTR ($P > 0.05$). Conversely, BAY treatment did not prevent demyelination and actually showed a further reduction in MBP area compared to both CTR ($q = 11.44$, ***P < 0.0001) and CPZ groups ($q = 3.453$, #P < 0.05). A similar pattern was observed in the cortex ($F(3,17) = 27.69$, $P < 0.0001$). CPZ administration significantly decreased myelin density ($q = 7.451$, ***P < 0.001), an effect that was completely reversed by PSB ($P > 0.05$ vs CTR; $q = 6.242$, ###P < 0.001 vs CPZ). Again, BAY60-6583 treated mice exhibited the lowest MBP levels, significantly different from all other groups (#P < 0.01 vs CPZ; ***P < 0.0001 vs CTR). In the striatum, although the overall effect was less pronounced, it remained significant ($F(3,17) = 6.904$, $P = 0.0030$). CPZ mice showed a significant reduction in MBP area ($q = 6.003$, **P < 0.01), which was significantly attenuated by PSB 603 ($q = 3.723$, #P < 0.05 vs CPZ), bringing the values back to CTR levels ($P > 0.05$). No

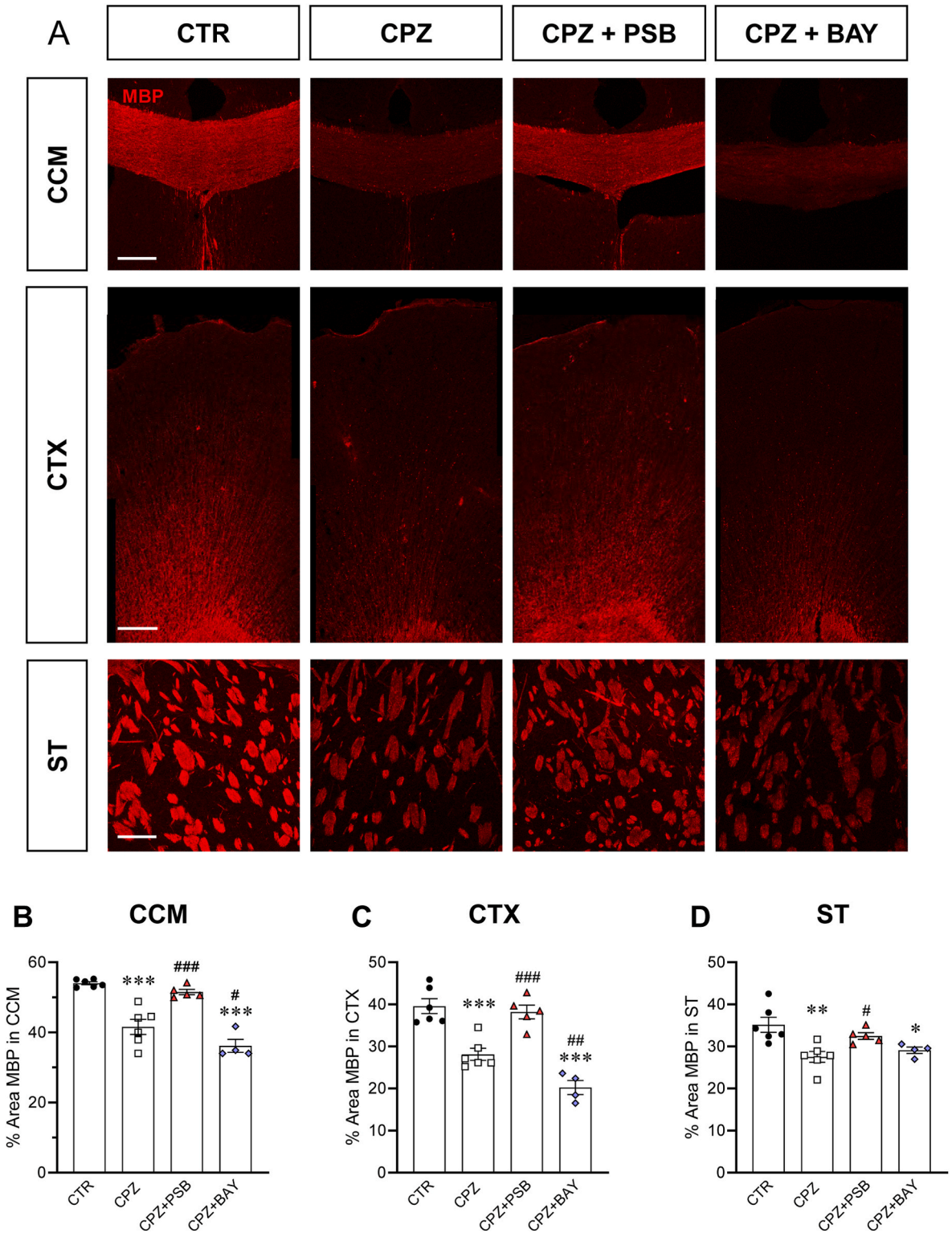

Fig. 5. Effect of A2BR modulation on MBP immunostaining in the CPZ demyelination model. **A:** Representative confocal images showing myelin basic protein (MBP) immunofluorescence in the corpus callosum medialis (CCM), motor cortex (CTX) and striatum (ST) in different experimental conditions. Scale bars: 200 μm. **B-D:** Quantitative analyses of the percentage of MBP-positive area (red) in CCM (B), CTX (C) and ST (D) in the four experimental groups: CPZ exposure induced a marked reduction of MBP immunofluorescence in all the regions investigated. Treatment with PSB significantly reverted CPZ effect in all regions investigated, while BAY60-6583 was not effective. *P < 0.05, **P < 0.01 and ***P < 0.001 vs CTR; #P < 0.05 and ##P < 0.01 vs CPZ (one-way ANOVA followed by Newman Keuls post hoc test). In all graphs data are expressed as mean ± SEM. CTR, n = 6; CPZ, n = 6; CPZ + PSB, n = 5; CPZ + BAY, n = 4. (For interpretation of the references to colour in this figure legend, the reader is referred to the Web version of this article.)

significant recovery was observed for the BAY60-6583 group in this region (P > 0.05 vs CPZ).

3.3. Effect of A2BR ligands on CPZ–induced astrocytes reactivity in corpus callosum medialis, cortex, and striatum

Astrocytes were immunostained with anti-GFAP antibody in brain sections of the four experimental group; CCM, CTX and ST were our regions of interest for confocal microscopy acquisitions. From the representative confocal images shown in Fig. 6A it is apparent that astrocytes were more numerous and more activated in the CCM of CPZ mice in comparison to CTR mice.

Fig. 6B shows the results of quantitative analyses of GFAP immunostaining in the CCM of the four experimental groups.n the CCM of CPZ-treated mice GFAP immunostaining increased in comparison to CTR mice, an indication that astrocytes were more activated. PSB 603 significantly reverted this effect, while BAY60-6583 further increased GFAP immunostaining: One-way ANOVA ($F(3,16) = 16.29$, $P < 0.0001$) and Newman-Keuls post hoc test: **P < 0.01 CPZ vs CTR (q = 5.610); ***P < 0.001 CPZ + BAY vs CTR (q = 9.298); #P < 0.05 CPZ + PSB vs CPZ (q = 3.361); ##P < 0.01 CPZ + BAY vs CPZ (q = 4.280). Fig. 6C shows that in the CCM of CPZ-treated mice astrocytes density increased significantly in comparison to CTR mice. PSB 603 slightly, although not significantly, reverted this effect, while BAY60-6583 slightly increased astrocytes density: one-way ANOVA ($F(3,16) = 9.578$, $P = 0.0007$) and Newman-Keuls post hoc test: *P < 0.05 CPZ vs CTR (q = 5927); **P < 0.01 CPZ + PSB vs CTR (q = 3.721); ***P < 0.001 CPZ + BAY vs CTR (q = 6.878).

The representative confocal images of GFAP immunohistochemistry in the cortex (Fig. 6A), show that astrocytes were more numerous and more activated in the cortex of CPZ mice in comparison to CTR mice.

Fig. 6D shows that in the cortex of CPZ-treated mice GFAP immunostaining significantly increased in comparison to CTR mice. PSB 603 completely reverted this effect. BAY60-6583 further increased, although slightly, GFAP immunostaining: one-way ANOVA ($F(3,17) = 10.29$, $P = 0.0004$) and Newman-Keuls post hoc test: *P < 0.05 CPZ vs CTR (q = 4.728); **P < 0.01 CPZ + BAY vs CTR (q = 6.579); ##P < 0.01 CPZ + PSB vs CPZ (q = 4.280). Fig. 6E shows that in the cortex of CPZ-treated mice astrocyte density significantly increased in comparison to CTR mice. PSB 603 significantly reverted this effect, while BAY60-6583 did not have any effect:ne-way ANOVA ($F(3,16) = 22.95$, $P < 0.0001$) and Newman-Keuls post hoc test: **P < 0.01 CPZ + PSB vs CTR (q = 4.300); ***P < 0.001 CPZ vs CTR (q = 10.91) and CPZ + BAY vs CTR (q = 8.426); ##P < 0.01, CPZ + PSB vs CPZ (q = 5.462).

The representative confocal images of GFAP immunohistochemistry in the striatum (Fig. 6A) show that astrocytes were more numerous and more activated in the striatum of CPZ mice compared to CTR mice.

The graphs in Fig. 6F shows that GFAP immunostaining in the striatum of CPZ-treated mice was significantly increased compared to CTR mice. PSB 603 completely reverted this effect, while BAY60-6583 had no effect:one-way ANOVA ($F(3,16) = 7.130$, $P = 0.0030$) and Newman-Keuls post hoc test: *P < 0.05 CPZ vs CTR (q = 4.531); **P < 0.01 CPZ + BAY vs CTR (q = 5.592); #P < 0.05, CPZ + PSB vs CPZ (q = 3.319). Fig. 6G shows that in the striatum of CPZ-treated mice there was a significant increase of astrocytes density compared to CTR mice. PSB 603 partially, although significantly, reverted the increase, while BAY 60-6883 did not have any effect:one-way ANOVA ($F(3,16) = 9.505$, $P = 0.0008$) and Newman-Keuls post hoc test: **P < 0.01 CPZ vs CTR (q = 6.130) and CPZ + BAY vs CTR (q = 6.652).

3.4. Effect of A2BR ligands on CPZ–induced microglia reactivity in corpus callosum medialis, cortex and striatum

Microglia were immunostained with anti-IBA1 antibody in brain sections of the four experimental groups. CCM, CTX and ST were our regions of interest for confocal microscopy acquisitions. From the representative confocal images shown in Fig. 7A it is apparent that microglia were more numerous and more activated in the CCM of CPZ mice than in CTR mice.

The graph in Fig. 7B shows that IBA1 immunostaining in the CCM of CPZ-treated mice was significantly increased in comparison to CTR mice. PSB 603 slightly but significantly reverted this increase, while BAY60-6583 did not change IBA1 immunostaining in comparison to CPZ mice. Statistical analysis: one-way ANOVA ($F(3,16) = 31.07$, $P < 0.0001$) and Newman-Keuls post hoc test: ***P < 0.001 CPZ vs CTR (q = 11.51), CPZ + PSB vs CTR (q = 6.694) and CPZ + BAY vs CTR (q = 11.71); #P < 0.05, CPZ + PSB vs CPZ (q = 3.604). Fig. 7C shows that in the CCM of CPZ-treated mice microglia density significantly increased in comparison to CTR mice. PSB 603 completely reverted this effect, while BAY60-6583 did not change microglia density in comparison to CPZ mice. Statistical analysis:one-way ANOVA ($F(3,16) = 12.45$, $P = 0.0002$) and Newman-Keuls post hoc test: **P < 0.01 CPZ vs CTR (q = 5.967); ***P < 0.001 CPZ + BAY vs CTR (q = 7.334); ##P < 0.01, CPZ + PSB vs CPZ (q = 4.484).

From the representative confocal images (Fig. 7A), it is apparent that microglia were more activated in the cortex of CPZ mice in comparison to CTR mice.

The graph in Fig. 7D show that IBA1 immunostaining show that in the cortex of CPZ-treated mice IBA1 immunostaining was slightly, but not significantly, increased compared to CTR mice. PSB 603 slightly reverted this effect. BAY60-6583 administration did not change IBA1 immunostaining in comparison to CPZ mice. Statistical analysis: one-way ANOVA ($F(3,17) = 2.522$, $P = 0.0923$) and Newman-Keuls post hoc test showed that there was no significant difference among the four experimental groups. Fig. 7E shows that in the cortex of CPZ-treated mice microglia density significantly increased in comparison to CTR mice. PSB 603 completely reverted this effect, while BAY60-6583 treatment had no effect in comparison to CPZ mice. Statistical analysis: one-way ANOVA ($F(3,17) = 3.926$, $P = 0.0268$) and Newman-Keuls post hoc test: *P < 0.05 CPZ vs CTR (q = 4.079); #P < 0.05 CPZ + PSB vs CPZ (q = 3.643).

Representative confocal images in Fig. 7A show that microglia were more numerous and more activated in the striatum of CPZ mice in comparison to CTR mice.

The graph in Fig. 7F shows tshows that in the striatum of CPZ-treated mice there was a significant increase in IBA1 immunostaining compared to CTR mice. PSB 603 completely reverted this effect, while BAY60-6583 did not change IBA1 immunostaining in comparison to CPZ mice. Statistical analysis:one-way ANOVA ($F(3,16) = 6.057$, $P = 0.0059$) and Newman-Keuls post hoc test: *P < 0.05 CPZ vs CTR (q = 3.170) and CPZ + BAY vs CTR (q = 4.307); #P < 0.05, CPZ + PSB vs CPZ (q = 4.144). Fig. 7G shows that in the striatum of CPZ-treated mice microglia density significantly increased in comparison to CTR mice. PSB 603 or BAY60-6583 did not revert this effect. Statistical analysis: one-way ANOVA ($F(3,17) = 3.464$, $P = 0.0396$) and Newman-Keuls post hoc test: *P < 0.05 CPZ vs CTR (q = 3.670) and CPZ + PSB vs CTR (q = 4.071).

4. Discussion

In the present study we assessed the potential protective role of A2BR modulation on CPZ-induced demyelination in the mouse, focusing on glial alterations associated with demyelinating damage, through the administration of PSB 603 or BAY60-6583. Our data demonstrate that the selective pharmacological blockade of A2BRs by PSB 603 exerted a protective effect, promoting myelin restoration in CCM, the primary site of CPZ-dependent demyelination in the brain, as well as in the CTX and ST. Since PSB603 was administered during the last two weeks of continuous CPZ exposure, the observed higher myelin density could result from an inhibition of myelin breakdown rather than active remyelination. Moreover, A2BR antagonism attenuated CPZ-dependent astrogliosis and microgliosis in the same brain regions.

The *in vivo* mouse model of CPZ-enriched diet represents a

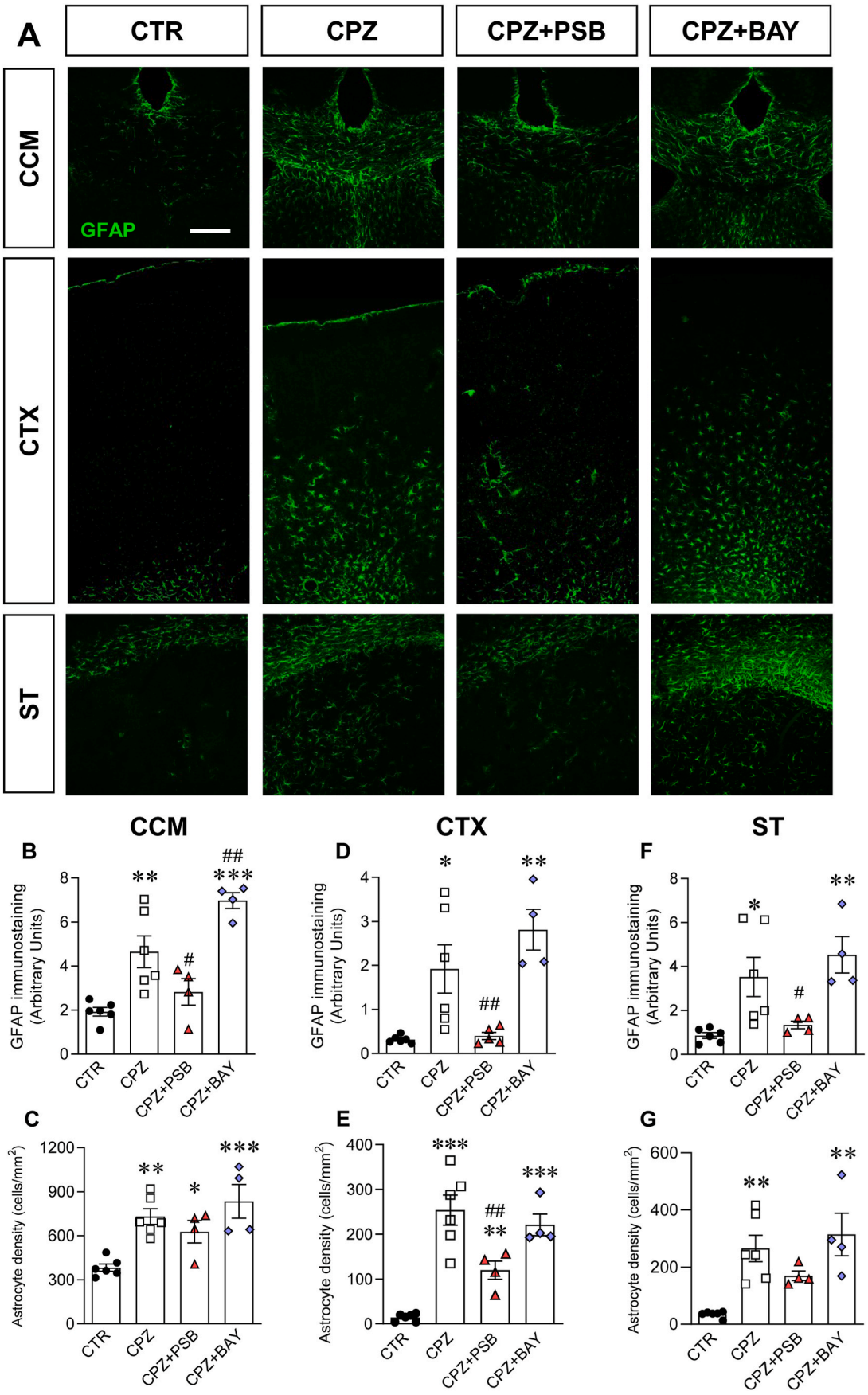

(caption on next page)

Fig. 6. Analysis of astrocytes in the corpus callosum medialis (CCM), in the cortex (CTX) and in the striatum (ST) of CTR, CPZ, CPZ + PSB, and CPZ + BAY mice. **A**: Representative confocal images of GFAP immunostaining of astrocytes (green) in CCM, CTX and ST of a CTR, a CPZ, a CPZ + PSB and a CPZ + BAY mouse. Scale bar: 150 μm. **B-C:** Quantitative analysis of GFAP immunostaining (arbitrary units) and GFAP + astrocyte density (cells/mm^2) in the CCM of each experimental group. **D-E:** Quantitative analysis of GFAP immunostaining (arbitrary units) andGFAP + astrocyte density (cells/mm^2) in CTX of each experimental group). **F-G:** Quantitative analysis of GFAP immunostaining (arbitrary units) andGFAP + astrocyte density (cells/mm^2) in ST of each experimental group. Data reported in all graph bars are expressed as mean ± SEM. CTR (n = 6), CPZ (n = 6), CPZ + PSB (n = 4) and CPZ + BAY mice (n = 4). (For interpretation of the references to colour in this figure legend, the reader is referred to the Web version of this article.)

substantiated tool for investigating demyelination processes in the brain. Research demonstrated that CPZ causes selective OLs apoptosis and subsequent demyelination without direct injury to OPCs and with minimal involvement of the immune/inflammatory systems in the process of disruption of the myelin sheet. For instance, Zoupi and coworkers highlighted that the CPZ model enables the study of demyelination and remyelination processes while largely excluding immune system contributions to demyelination, making it an ideal tool to investigate direct OLs cytotoxicity (Zoupi et al., 2013). Indeed, as a copper chelator, CPZ selectively targets OLs inducing their apoptosis and triggering demyelination, predominantly in the corpus callosum (Gingele et al., 2020), but also in the striatum and cortex. After CPZ relief, OPCs are described to migrate to the lesion site and to differentiate into mature OLs triggering remyelination processes restoring myelin levels. This model provides valuable insight into the distinct responses of mature OLs and OPCs to CPZ-induced intoxication. Buschmann and colleagues reported that the selective OL death and decline in myelin-related genes expression occur rapidly after the onset of CPZ exposure, well before overt demyelination (Buschmann et al., 2012).

Adenosine signaling plays a critical role in CPZ-induced demyelination. The activation of adenosine receptors has been shown to modulate the inflammatory response and support OLs survival during demyelination (Adebiyi and Bynoe, 2023). Evidence suggests that enhanced adenosine signaling through A1 receptors can promote OLs survival and facilitate in vitro myelination (Stevens et al., 2002), highlighting the relevance of targeting adenosine pathway as a therapeutic approach for demyelinating diseases (Adebiyi and Bynoe, 2023).

The A2BR subtype, coupled to Gs protein, is considered the most enigmatic as its pharmacological and physiological properties have long been challenging to study due to the absence of selective ligands and its low affinity for the endogenous ligand adenosine (Coppi et al., 2020). The role of this receptor subtype in oligodendrogliogenesis remains poorly understood. Recently, we demonstrated that A2BR activation inhibits OPC differentiation in vitro (Cherchi et al., 2024; Coppi et al., 2020). In particular, the A2BR agonist BAY60-6583 reversibly suppresses tetraethylammonium (TEA)-sensitive sustained IK and 4-aminopyridine (4-AP)-sensitive transient IA conductances (Coppi et al., 2020). It is well established that these currents are essential for OPC differentiation, and their modulation could serve as a valuable therapeutic target in demyelinating pathologies (Cherchi et al., 2021a; Chittajallu et al., 2004; Gallo et al., 1996; Yuan et al., 2002). The temporal dynamics of adenosine levels during CPZ treatment remain largely unexplored. However, it is hypothesized that adenosine levels fluctuate between the demyelinating phase typical of MS. During the acute phase of CPZ exposure, which leads to demyelination (Buschmann et al., 2012), an increase in adenosine levels may occur. As already mentioned, A2BRs are predominantly recruited under pathological conditions due to their low affinity for the endogenous ligand, and play a critical and controversial role in regulating OL survival and maintaining myelin integrity (Cherchi et al., 2024). Moreover, it has been demonstrated in cultured astroglial cells that A2BRs desensitize in a time dependent manner (Trincavelli et al., 2008) as a putative cell defense mechanism to counteract the A2BR-mediated effects during the acute phase of brain damage.

CPZ intake has been associated with a significant reduction in body weight. In accordance with literature (Ye et al., 2013; Krauthausen et al., 2014), mice exposed to CPZ showed a marked reduction in weight gain that became significant within three weeks. This result suggests that CPZ induced a reduction in food intake or may have a direct effect on fat metabolism and distribution even if the pathophysiological mechanisms of the toxin are not yet defined. The decrease in body weight variation persisted during the 2-weeks of pharmacological treatment. However, neither PSB 603 nor BAY60-6583 significantly modified weight decrease in CPZ-treated mice, suggesting that modulation of the A2BR does not have major influence on body weight changes. In research conducted by D'Antongiovanni et al., BAY60-6583 was shown to modulate metabolic pathways, leading to reductions in cholesterol and triglycerides levels, key factors in managing obesity-related cardiovascular diseases (D'Antongiovanni et al., 2021). BAY60-6583 could influence weight changes independently of the toxic effects of CPZ. However, as A2BRs are known to have a role in obesity, a direct effect of A2BR ligands on lipid metabolism cannot be excluded, leading to possible interference with body weight changes during or after CPZ treatment. The lack of effect of the A2BRs ligands is possibly due to the dominant toxic effect of CPZ that masks potential metabolic changes.

Consistent with previous findings (Zhang et al., 2020), behavioural tests further confirmed that CPZ exposure induced several motor alterations. In particular, the Hole-board test revealed in CPZ-fed mice a longer time spent in the center of the arena.This effect may be considered either an index of increased avoidance of the perimeter of the arena (source of fear for the mouse) or a consequence of a reduced mobility after toxin intake. Surprisingly, behavioural outcomes revealed that both groups of mice treated with PSB 603 or BAY60-6580 spent more time in the center of the arena. Exploratory activity, defined as the number of episodes in which the animal moved its head within the holes in the arena, was not significantly affected by the CPZ treatment. Furthermore, locomotor impairment is a key feature of CPZ treatment which correlates with OLs depletion. Khodanovich reported that 10 weeks CPZ treatment led to decreased locomotion (Khodanovich et al., 2019), aligning with findings from earlier studies. In 2012, Magalon et al. specifically reported that mice exhibit significant impairment in motor coordination during CPZ treatment, as measured by the Rotarod test (Magalon et al., 2012). Here we demonstrated that CPZ induced significant alteration of locomotor activity in the Hole-board test. In the CPZ treated mice, administration of PSB 603 or BAY60-6583 was able to prevent this deficit, restoring locomotion to control levels. To corroborate these findings, we performed the Rotarod test and, as expected, we found that CPZ-treated mice had a significantly shorter latency to the first fall. However, neither PSB 603 nor BAY60-6583 were able to recover this deleterious effect brought about by CPZ treatment. It is possible that motor coordination, balance, and grip, necessary to perform the Rotarod test, are coordinated by a system that does not necessitate of the adenosinergic system through A2BR.

In this context, it is known that adenosine levels and signalling play a critical role in demyelination. In particular, adenosine is a key regulator of oligodendrogliogenesis, exerting receptor-specific actions on OPC proliferation and differentiation (Cherchi et al., 2021b; Fields and Burnstock, 2006; Stevens et al., 2002). In line with the literature, immunohistochemical analyses in our study confirmed extensive demyelination in different brain regions of CPZ-treated mice, with significant reduction of MBP expression in CCM, CTX and ST (Buschmann et al., 2012; Guglielmetti et al., 2016; Tanaka et al., 2013). Importantly, we found that PSB 603 rescued myelin damaged induced by CPZ in all brain areas examined, consistent with reports showing that A2BR blockade preserves myelin integrity and improves clinical outcomes in

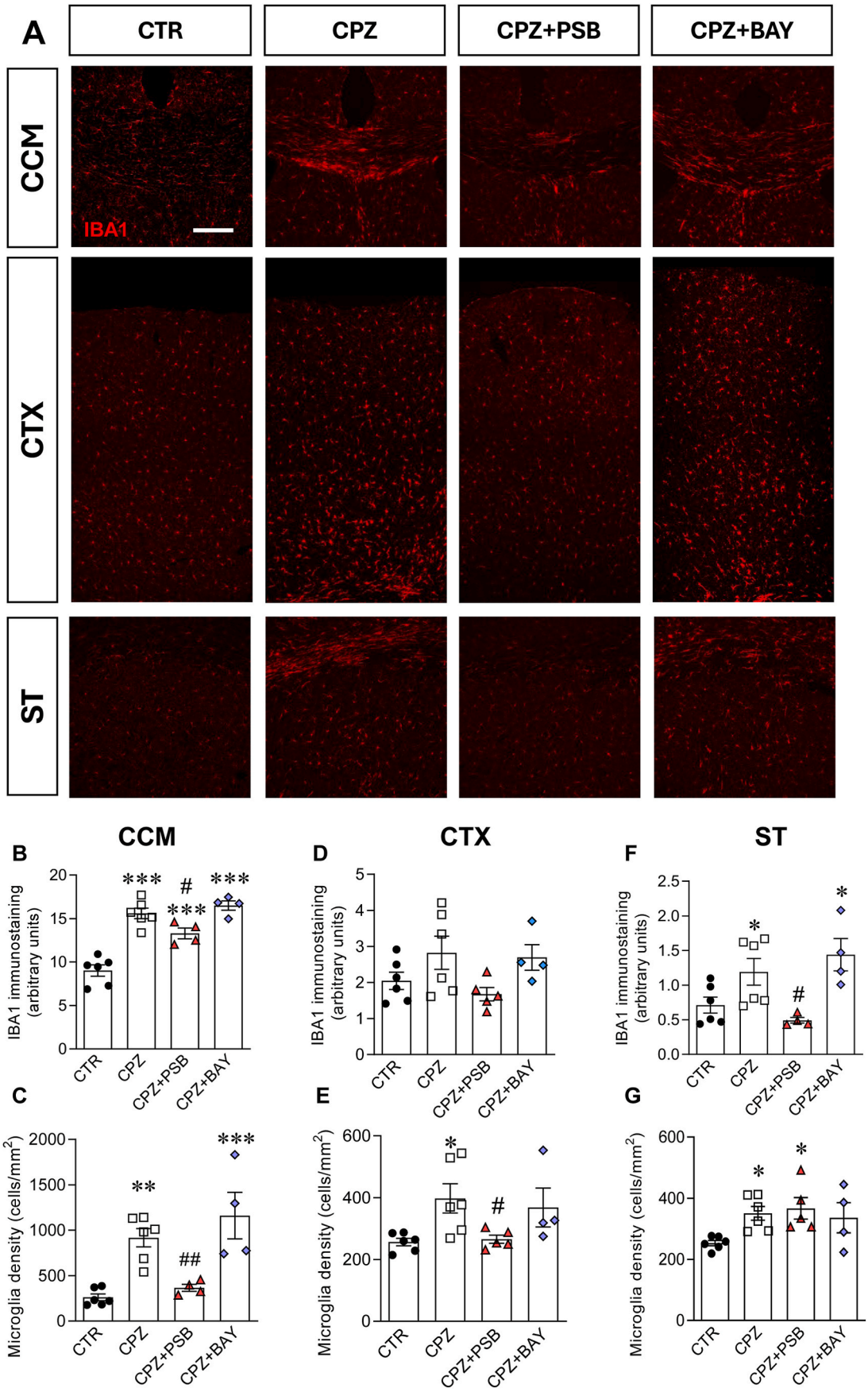

(caption on next page)

Fig. 7. Analysis of microglia in the corpus callosum medialis (CCM), in the cortex (CTX) and in the striatum (ST) of CTR, CPZ, CPZ + PSB, and CPZ + BAY mice. **A:** Representative confocal images of IBA1 immunostaining of microglia (red) in the CCM, CTX and ST of a CTR, a CPZ, a CPZ + PSB and a CPZ + BAY mouse. Scale bar: 150 μm. **B-C:** Quantitative analysis of IBA1 immunostaining (arbitrary units) and IBA1+ microglia density (cells/mm^2) in the CCM of each experimental group. **D-E:** Quantitative analysis of IBA1 immunofluorescence (arbitrary units) and IBA1+ microglia density (cells/mm^2) in the CTX of each experimental group. **F-G:** Quantitative analysis of IBA1 immunostaining (arbitrary units) andIBA1+ microglia density (cells/mm^2) in the ST of each experimental group. Data reported in all graph bars are expressed as mean ± SEM. CTR (n = 6), CPZ (n = 6), CPZ + PSB (n = 4-5), and CPZ + BAY mice (n = 4). (For interpretation of the references to colour in this figure legend, the reader is referred to the Web version of this article.)

demyelinating conditions such as EAE (Wei et al., 2013).

We found a significant increase in astrocyte density and GFAP immunofluorescence in the three ROIs following exposure to CPZ, in line with previous findings that report strong astrogliosis in CPZ-treated mice (Buonvicino et al., 2021; Matsushima and Morell, 2001; Skripuletz et al., 2008) a hallmark of the demyelinating process. Single-cell RNA sequencing (RNA-seq) data from the mouse brain (Zeisel et al., 2018) show that *Adora2b,* one of the two paralogous genes *Adora2a* and *Adora2b,* is strongly expressed in astrocytes, consistent with the recently published evidence indicating the A2B receptor as one of the highly expressed G protein-coupled receptors in astrocytes in the brain (Endo et al., 2022). On the contrary, the RNA-seq data suggest that astrocytes do not express *Adora2a* gene.

Treatment with PSB 603 significantly reduced activation and increased density of astrocytes induced by CPZ, whereas BAY60-6583 had no significant effect or tended to further increase astrocytes activation, especially in the CCM. The significant attenuation of astrocytes activation by PSB 603 is consistent with studies showing that A2BR signaling participates in astrocyte metabolic and reactive responses (Endo et al., 2022; Theparambil et al., 2024), indicating that blocking this receptor may modulate astrocytes reactivity. Indeed, metabolic activation of astrocytes is mediated by adenosine acting on astrocytic A2BRs, and knockdown of A2BRs in astrocytes leads to a major reprogramming of brain energy metabolism (Theparambil et al., 2024). During aging, progressive impairment of brain energy homeostasis may contribute to the development of neurodegenerative diseases (Cunnane et al., 2020) and treatments that can rescue and preserve brain energetics may prove effective in counteracting them. Modulation of A2BRs in brain astrocytes could potentially be an effective therapeutic strategy to support brain energy metabolism to promote brain longevity. There is increasing evidence that astrocytes are key players in complex interactions with OPC, mature oligodendrocytes, and microglia supporting remyelination at least in the CPZ model.

The clearance of myelin debris by microglia phagocytosis from the site of demyelination is important to achieve adequate remyelination and to slow the progression of the disease. Microglia activation is a well-characterized feature of the CPZ model (Hiremath et al., 1998a; Mason et al., 2004), where it plays a dual role, being essential for debris clearance and remyelination. However, how microglia phagocytose the myelin debris, and why their clearance is impaired in MS, is not fully known. Furthermore, there is continuous debate whether microglia play a deleterious or beneficial role in CNS diseases (Schwartz et al., 2006; Block et al., 2007; Hanisch and Kettenmann, 2007; Boche et al., 2013; Chhor et al., 2013).

Our results suggest that A2BR antagonism may exert a modulatory effect on microglia reactivity, potentially creating a more favourable environment for repair. In primary murine microglia the A2BR stimulates microglia proliferation and increases the production of both anti-inflammatory IL-10 and pro-inflammatory IL-6 cytokines (Fiebich et al., 1996; Koscsó et al., 2012; Merighi et al., 2017). These results are consistent with previous research, which demonstrates the role of adenosine receptors in the regulation of neuroinflammation and glial responses (Cherchi et al., 2021b; Coppi et al., 2020), and that pharmacological blockade of A2BRs prevents myelin disruption and neurological impairment in demyelinating models (Manalo et al., 2020; Wei et al., 2013). In the healthy adult brain, the phenomic of microglia as well as their distribution varies between different brain regions (Lana et al., 2023). In line with these data, the extent of microglia accumulation during CPZ-induced demyelination is not uniform among brain structures. These differences in microglia phenomic may explain the differential effects of the adenosinergic drugs we found. Likely due to the higher amount of myelin content/debris, a significantly stronger microgliosis can be observed in the white matter as compared to the gray matter (Skripuletz et al., 2008; Gudi et al., 2009).

Since so far no clear expression of A2BR has been demonstrated in microglia, the possibility exists that the effects of the adenosinergic drugs we observed are not direct on microglia, but may be secondary to their effect on astrocytes. Indeed, astrocytes play an important role in the phagocytic process by recruiting microglia to the site of demyelination and producing regenerative mediators (Sen et al., 2022).

This study confirms that the CPZ model reproduces many of the pathological hallmarks of demyelination, including impaired weight gain, behavioural deficits, astrogliosis, microglial activation (Hiremath et al., 1998b; Mason et al., 2004; Sen et al., 2022; Skripuletz et al., 2011). These results are consistent with previous researches, implicating adenosine receptors in the regulation of neuroinflammation and glial responses (Cherchi et al., 2021b; Coppi et al., 2020), and they align with studies demonstrating that pharmacological blockade of A2BRs prevents myelin disruption and neurological impairment in demyelinating models (Manalo et al., 2020; Wei et al., 2013). It is known that PSB 603 crosses the blood brain barrier (Lindemann et al., 2021). However, we cannot exclude that at least part of the effects of the drugs used are due to their possible peripheral actions.

In order to explain the discrepancy between behavioral responses and immunohistochemistry results following A2BR ligands administration, we hypothesized that chronic A2BR stimulation could induce a receptor desensitization leading to a similar response between BAY60-6583 and the antagonist PSB 603. In addition, it is important underlying that a different cellular localization of A2BR may subtend the similar response induced by both agonist and antagonist, accordingly to Cherchi and coll. (Cherchi et al., 2024). Finally, we may hypothesize that BAY60-6583 restorative effect on spontaneous mobility is due to an integrated action on unexamined brain/cortical areas that govern and regulate associative, exploratory/motivational behavior. The effect of BAY60-6583 on these areas may lead to compensation for the myelin deficit caused by CPZ.

Overall, our findings highlight the potential of A2BR antagonism as therapeutic tool in demyelinating disorders in line with emerging literature, suggesting that targeting adenosine signaling may promote oligodendrocyte survival, remyelination, and neuroprotection (Cherchi et al., 2024; Coppi et al., 2020), although further experiments are needed to better understand the complexity of adenosinergic signaling in the process of demyelination.

Declaration of generative AI and AI-assisted technologies in the manuscript preparation process

During the preparation of this work the authors used Notebooklm in order to create the background image of the graphical abstract. After using this tool, the authors reviewed and edited the content as needed and took full responsibility for the content of the publication.

Funding information

The research was funded by.

- Università degli Studi di Firenze, Grant/Award Number: RICATEN: **AMP, MGG, EC, DL.**
- Next Generation European Union, in the context of the National Recovery and Resilience Plan, M4C2 Investment 1.5 (THE - Tuscany Health Ecosystem), CUP B83C22003920001: **AMP.**
- National Recovery and Resilience Plan M4C2 Investment 1.4 (CN00000041 CN3 "National Center for Gene Therapy and Drugs based on RNA Technology" Spoke #3 CUP:13C22001010001): **AMP, MGG.**
- FISM – Fondazione Italiana Sclerosi Multipla – cod. 2024/R-Single/038 and financed or co-financed with the '5per mille' public founding: **EC.**
- Daniele Lana current position is supported by #NEXTGENERATIONEU (NGEU) and funded by the Ministry of University and Research (MUR), National Recovery and Resilience Plan (NRRP), project MNESYS (PE0000006) (DR. 1553 11.10.2022): **DL.**

CRediT authorship contribution statement

Federica Cherchi: Conceptualization, Data curation, Investigation, Methodology, Supervision, Visualization, Writing – original draft, Writing – review & editing. **Martina Venturini:** Conceptualization, Data curation, Investigation, Methodology, Supervision, Visualization, Writing – original draft, Writing – review & editing. **Lucia Frulloni:** Data curation, Investigation, Methodology. **Federica Panozzi:** Data curation, Investigation, Methodology. **Giada Magni:** Formal analysis, Methodology. **Clara Santalmasi:** Formal analysis, Methodology. **Camilla Maestrelli:** Formal analysis, Methodology. **Maria Grazia Giovannini:** Funding acquisition, Supervision, Writing – original draft, Writing – review & editing. **Elisabetta Coppi:** Funding acquisition, Supervision, Writing – review & editing. **Daniele Lana:** Conceptualization, Data curation, Funding acquisition, Supervision, Writing – review & editing. **Anna Maria Pugliese:** Conceptualization, Data curation, Funding acquisition, Resources, Supervision, Writing – review & editing.

Declaration of competing interest

The authors declare that they have no known competing financial interests or personal relationships that could have appeared to influence the work reported in this paper.

Acknowledgments

Confocal microscopy acquisitions were carried out at the Cnr—Istituto di Fisica Applicata "Nello Carrara," (Florence, Italy).

References

Adebiyi, O.E., Bynoe, M.S., 2023. Roles of adenosine receptor (subtypes A1 and A2A) in cuprizone-induced hippocampal demyelination. Mol. Neurobiol. 60, 5878–5890. https://doi.org/10.1007/S12035-023-03440-6.

Block, M.L., Zecca, L., Hong, J.S., 2007. Microglia-mediated neurotoxicity: uncovering the molecular mechanisms. Nat. Rev. Neurosci. 8, 57–69. https://doi.org/10.1038/nrn2038.

Boche, D., Perry, V.H., Nicoll, J.A., 2013. Review: activation patterns of microglia and their identification in the human brain. Neuropathol. Appl. Neurobiol. 39, 3–18. https://doi.org/10.1111/nan.12011.

Bot, Ilze, de Vries, Henk, Korporaal, Suzanne J.A., Foks, Amanda C., Bot, Martine, et al., 2012. Adenosine A2B Receptor Agonism Inhibits Neointimal Lesion Development After Arterial Injury in Apolipoprotein E–Deficient Mice. Arteriosclerosis, Thrombosis, and Vascular Biology 32 (9), 2197–2205. https://doi.org/10.1161/atvbaha.112.252924. https://www.ahajournals.org/doi/10.1161/ATVBAHA.112.252924.

Buonvicino, D., Ranieri, G., Chiarugi, A., 2021. Cuprizone-dependent De/Remyelination responses and functional correlates in mouse strains adopted to model relapsing, chronic and progressive experimental autoimmune encephalomyelitis. Neurotox. Res. 39, 658–666. https://doi.org/10.1007/S12640-021-00331-3.

Buschmann, J.P., Berger, K., Awad, H., Clarner, T., Beyer, C., Kipp, M., 2012. Inflammatory response and chemokine expression in the white matter corpus callosum and gray matter cortex region during cuprizone-induced demyelination. J. Mol. Neurosci. 48, 66–76. https://doi.org/10.1007/S12031-012-9773-X.

Cherchi, F., Bulli, I., Venturini, M., Pugliese, A.M., Coppi, E., 2021a. Ion channels as new attractive targets to improve Re-Myelination processes in the brain. Int. J. Mol. Sci. 22. https://doi.org/10.3390/IJMS22147277.

Cherchi, F., Pugliese, A.M., Coppi, E., 2021b. Oligodendrocyte precursor cell maturation: role of adenosine receptors. Neural Regen. Res. 16, 1686–1692. https://doi.org/10.4103/1673-5374.306058.

Cherchi, F., Venturini, M., Magni, G., Frulloni, L., Chieca, M., Buonvicino, D., Santalmasi, C., Rossi, F., De Logu, F., Coppi, E., Pugliese, A.M., 2024. Adenosine A2B receptors differently modulate oligodendrogliogenesis and myelination depending on their cellular localization. Glia 72, 1985–2000. https://doi.org/10.1002/GLIA.24593.

Chhor, V., Le Charpentier, T., Lebon, S., Oré, M.V., Celador, I.L., Josserand, J., Degos, V., Jacotot, E., Hagberg, H., Sävman, K., Mallard, C., Gressens, P., Fleiss, B., 2013. Characterization of phenotype markers and neuronotoxic potential of polarised primary microglia in vitro. Brain Behav. Immun. 32, 70–85. https://doi.org/10.1016/j.bbi.2013.02.005.

Chittajallu, R., Aguirre, A., Gallo, V., 2004. NG2-positive cells in the mouse white and grey matter display distinct physiological properties. J. Physiol. 561, 109–122. https://doi.org/10.1113/JPHYSIOL.2004.074252.

Coppi, E., Dettori, I., Cherchi, F., Bulli, I., Venturini, M., Lana, D., Giovannini, M.G., Pedata, F., Pugliese, A.M., 2020. A2B adenosine receptors: when outsiders may become an attractive target to treat brain ischemia or demyelination. Int. J. Mol. Sci. 21, 1–14. https://doi.org/10.3390/IJMS21249697.

Coppi, E., Dettori, I., Cherchi, F., Bulli, I., Venturini, M., Pedata, F., Pugliese, A.M., 2021. New insight into the role of adenosine in demyelination, stroke and neuropathic pain. Front. Pharmacol. 11, 625662. https://doi.org/10.3389/fphar.2020.625662.

Cunnane, S.C., Trushina, E., Morland, C., Prigione, A., Casadesus, G., Andrews, Z.B., Beal, M.F., Bergersen, L.H., Brinton, R.D., de la Monte, S., Eckert, A., Harvey, J., Jeggo, R., Jhamandas, J.H., Kann, O., la Cour, C.M., Martin, W.F., Mithieux, G., Moreira, P.I., Murphy, M.P., Nave, K.A., Nuriel, T., Oliet, S.H.R., Saudou, F., Mattson, M.P., Swerdlow, R.H., Millan, M.J., 2020. Brain energy rescue: an emerging therapeutic concept for neurodegenerative disorders of ageing. Nat. Rev. Drug Discov. 19, 609–633. https://doi.org/10.1038/S41573-020-0072-X.

D'Antongiovanni, Vanessa, Fornai, Matteo, Pellegrini, Carolina, Blandizzi, Corrado, Antonioli, Luca, 2021. Managing Obesity and Related Comorbidities: A Potential Pharmacological Target in the Adenosine System? Frontiers in Pharmacology 11, 621955. https://doi.org/10.3389/fphar.2020.621955. https://www.frontiersin.org/articles/10.3389/fphar.2020.621955/full. (Accessed 18 January 2021).

Dettori, Ilaria, Gaviano, Lisa, Ugolini, Filippo, Lana, Daniele, Bulli, Irene, et al., 2021. Protective Effect of Adenosine A2B Receptor Agonist, BAY60-6583, Against Transient Focal Brain Ischemia in Rat. Frontiers in Pharmacology 11, 588757. https://doi.org/10.3389/fphar.2020.588757. https://www.frontiersin.org/articles/10.3389/fphar.2020.588757/full. (Accessed 11 February 2021).

Eckle, Tobias, Faigle, Marion, Grenz, Almut, Laucher, Stefanie, Thompson, Linda F., et al., 2008. A2B adenosine receptor dampens hypoxia-induced vascular leak. Blood 111 (4), 2024–2035. https://doi.org/10.1182/blood-2007-10-117044. https://ashpublications.org/blood/article/111/4/2024/133338/A2B-adenosine-receptor-dampens-hypoxiainduced.

Endo, F., Kasai, A., Soto, J.S., Yu, X., Qu, Z., Hashimoto, H., Gradinaru, V., Kawaguchi, R., Khakh, B.S., 2022. Molecular basis of astrocyte diversity and morphology across the CNS in health and disease. Science 378. https://doi.org/10.1126/science.adc9020.

Fiebich, B.L., Biber, K., Gyufko, K., Berger, M., Bauer, J., Van Calker, D., 1996. Adenosine A2b receptors mediate an increase in interleukin (IL)-6 mRNA and IL-6 protein synthesis in human astroglioma cells. J. Neurochem. 66, 1426–1431. https://doi.org/10.1046/J.1471-4159.1996.66041426.X.

Fields, R.D., Burnstock, G., 2006. Purinergic signalling in neuron-glia interactions. Nat. Rev. Neurosci. 7, 423–436. https://doi.org/10.1038/NRN1928.

Fredholm, B.B., Ijzerman, A.P., Jacobson, K.A., Linden, J., Müller, C.E., 2011. International union of basic and clinical pharmacology. LXXXI. Nomenclature and classification of adenosine receptors - an update. Pharmacol. Rev. 63, 1–34. https://doi.org/10.1124/pr.110.003285.

Fusco, I., Ugolini, F., Lana, D., Coppi, E., Dettori, I., Gaviano, L., Nosi, D., Cherchi, F., Pedata, F., Giovannini, M.G., Pugliese, A.M., 2018. The selective antagonism of adenosine A2B receptors reduces the synaptic failure and neuronal death induced by oxygen and glucose deprivation in rat CA1 hippocampus in vitro. Front. Pharmacol. 9. https://doi.org/10.3389/FPHAR.2018.00399.

Galeotti, N., Sanna, M.D., Ghelardini, C., 2013. Pleiotropic effect of histamine H4 receptor modulation in the central nervous system. Neuropharmacology 71, 141–147. https://doi.org/10.1016/j.neuropharm.2013.03.026.

Gallo, V., Zhou, J.M., McBain, C.J., Wright, P., Knutson, P.L., Armstrong, R.C., 1996. Oligodendrocyte progenitor cell proliferation and lineage progression are regulated by glutamate receptor-mediated K+ channel block. J. Neurosci. 16, 2659–2670. https://doi.org/10.1523/JNEUROSCI.16-08-02659.1996.

Gingele, S., Henkel, F., Heckers, S., Moellenkamp, T.M., Hümmert, M.W., Skripuletz, T., Stangel, M., Gudi, V., 2020. Delayed demyelination and impaired remyelination in aged mice in the cuprizone model. Cells 9. https://doi.org/10.3390/CELLS9040945.

Giovannini, M.G., 2002. Double-label confocal microscopy of phosphorylated protein kinases involved in long-term potentiation. Methods Enzymol. 345, 426–436. https://doi.org/10.1016/S0076-6879(02)45035-5.

Gudi, V., Moharregh-Khiabani, D., Skripuletz, T., Koutsoudaki, P.N., Kotsiari, A., Skuljec, J., Trebst, C., Stangel, M., 2009. Regional differences between grey and white matter in cuprizone induced demyelination. Brain Res. 1283, 127–138. https://doi.org/10.1016/j.brainres.2009.06.005.

Guglielmetti, C., Veraart, J., Roelant, E., Mai, Z., Daans, J., Van Audekerke, J., Naeyaert, M., Vanhoutte, G., Delgado y Palacios, R., Praet, J., Fieremans, E., Ponsaerts, P., Sijbers, J., Van der Linden, A., Verhoye, M., 2016. Diffusion kurtosis imaging probes cortical alterations and white matter pathology following cuprizone induced demyelination and spontaneous remyelination. Neuroimage 125, 363–377. https://doi.org/10.1016/j.neuroimage.2015.10.052.

Hanisch, U.K., Kettenmann, H., 2007. Microglia: active sensor and versatile effector cells in the normal and pathologic brain. Nat. Neurosci. 10, 1387–1394. https://doi.org/10.1038/nn1997.

Hiremath, M.M., Saito, Y., Knapp, G.W., Ting, J.P.Y., Suzuki, K., Matsushima, G.K., 1998a. Microglial/macrophage accumulation during cuprizone-induced demyelination in C57BL/6 mice. J. Neuroimmunol. 92, 38–49. https://doi.org/10.1016/S0165-5728(98)00168-4.

Hiremath, M.M., Saito, Y., Knapp, G.W., Ting, J.P.Y., Suzuki, K., Matsushima, G.K., 1998b. Microglial/macrophage accumulation during cuprizone-induced demyelination in C57BL/6 mice. J. Neuroimmunol. 92, 38–49. https://doi.org/10.1016/S0165-5728(98)00168-4.

Khodanovich, M., Pishchelko, A., Glazacheva, V., Pan, E., Akulov, A., Svetlik, M., Tyumentseva, Y., Anan'Ina, T., Yarnykh, V., 2019. Quantitative imaging of white and gray matter remyelination in the cuprizone demyelination model using the macromolecular Proton fraction. Cells 8. https://doi.org/10.3390/CELLS8101204.

Kornguth, S.E., Anderson, J.W., 1965. Localization of a basic protein in the myelin of various species with the aid of fluorescence and electron microscopy. J. Cell Biol. 26, 157–166. https://doi.org/10.1083/JCB.26.1.157.

Koscsó, B., Csóka, B., Selmeczy, Z., Himer, L., Pacher, P., Virág, L., Haskó, G., 2012. Adenosine augments IL-10 production by microglial cells through an A2B adenosine receptor-mediated process. J. Immunol. 188, 445–453. https://doi.org/10.4049/JIMMUNOL.1101224.

Krauthausen, M., Saxe, S., Zimmermann, J., Emrich, M., Heneka, M.T., Müller, M., 2014. CXCR3 modulates glial accumulation and activation in cuprizone-induced demyelination of the central nervous system. J. Neuroinflammation 11, 109. https://doi.org/10.1186/1742-2094-11-109.

Laatsch, R.H., Kies, M.W., Gordon, S., Alvord, E.C., 1962. The encephalomyelitic activity of myelin isolated by ultracentrifugation. J. Exp. Med. 115, 777–788. https://doi.org/10.1084/JEM.115.4.777.

Lana, D., Magni, G., Landucci, E., Wenk, G.L., Pellegrini-Giampietro, D.E., Giovannini, M. G., 2023. Phenomic microglia diversity as a druggable target in the hippocampus in neurodegenerative diseases. Int. J. Mol. Sci. 24, 13668. https://doi.org/10.3390/ijms241813668.

Lana, D., Melani, A., Pugliese, A.M., Cipriani, S., Nosi, D., Pedata, F., Giovannini, M.G., 2014. The neuron-astrocyte-microglia triad in a rat model of chronic cerebral hypoperfusion: protective effect of dipyridamole. Front. Aging Neurosci. 6. https://doi.org/10.3389/fnagi.2014.00322.

Lana, D., Traini, C., Bulli, I., Sarti, G., Magni, G., Attorre, S., Giovannini, M.G., Vannucchi, M.G., 2024. Chronic administration of prebiotics and probiotics ameliorates pathophysiological hallmarks of Alzheimer's disease in a APP/PS1 transgenic mouse model. Front. Pharmacol. 15, 1451114. https://doi.org/10.3389/fphar.2024.1451114.

Lindemann, M., Dukic-Stefanovic, S., Hinz, S., Deuther-Conrad, W., Teodoro, R., Juhl, C., Steinbach, J., Brust, P., Müller, C.E., Wenzel, B., 2021. Synthesis of novel fluorinated xanthine derivatives with high adenosine A2B receptor binding affinity. Pharmaceuticals 14, 485. https://doi.org/10.3390/ph14050485.

Magalon, K., Zimmer, C., Cayre, M., Khaldi, J., Bourbon, C., Robles, I., Tardif, G., Viola, A., Pruss, R.M., Bordet, T., Durbec, P., 2012. Olesoxime accelerates myelination and promotes repair in models of demyelination. Ann. Neurol. 71, 213–226. https://doi.org/10.1002/ANA.22593.

Manalo, J.M., Liu, H., Ding, D., Hicks, J., Sun, H., Salvi, R., Kellems, R.E., Pereira, F.A., Xia, Y., 2020. Adenosine A2B receptor: a pathogenic factor and a therapeutic target for sensorineural hearing loss. FASEB J. 34, 15771–15787. https://doi.org/10.1096/FJ.202000939R.

Mason, J.L., Toews, A., Hostettler, J.D., Morell, P., Suzuki, K., Goldman, J.E., Matsushima, G.K., 2004. Oligodendrocytes and progenitors become progressively depleted within chronically demyelinated lesions. Am. J. Pathol. 164, 1673–1682. https://doi.org/10.1016/S0002-9440(10)63726-1.

Matsushima, G.K., Morell, P., 2001. The neurotoxicant, cuprizone, as a model to study demyelination and remyelination in the central nervous system. Brain Pathol. 11, 107–116. https://doi.org/10.1111/J.1750-3639.2001.TB00385.X.

Mercatelli, R., Lana, D., Bucciantini, M., Giovannini, M.G., Cerbai, F., Quercioli, F., Zecchi-Orlandini, S., Delfino, G., Wenk, G.L., Nosi, D., 2016. Clasmatodendrosis and b-amyloidosis in aging hippocampus. FASEB J. 30, 1480–1491. https://doi.org/10.1096/fj.15-275503.

Merighi, S., Bencivenni, S., Vincenzi, F., Varani, K., Borea, P.A., Gessi, S., 2017. A2B adenosine receptors stimulate IL-6 production in primary murine microglia through p38 MAPK kinase pathway. Pharmacol. Res. 117, 9–19. https://doi.org/10.1016/j.phrs.2016.11.024.

Pedata, F., Dettori, I., Coppi, E., Melani, A., Fusco, I., Corradetti, R., Pugliese, A.M., 2016. Purinergic signalling in brain ischemia. Neuropharmacology 104, 105–130. https://doi.org/10.1016/j.neuropharm.2015.11.007.

Sarti, G., Traini, C., Magni, G., Attorre, S., Tognozzi, G., Calussi, E., Giovannini, M.G., Vannucchi, M.G., Lana, D., 2025. Chronic administration of prebiotics and probiotics prevent pathophysiological hallmarks of Alzheimer's disease in the cortex of APP/PS1 mice. Front. Pharmacol. 16, 1596469. https://doi.org/10.3389/fphar.2025.1596469.

Schwartz, M., Butovsky, O., Brück, W., Hanisch, U.K., 2006. Microglial phenotype: is the commitment reversible? Trends Neurosci. 29, 68–74. https://doi.org/10.1016/j.tins.2005.12.005.

Sen, M.K., Mahns, D.A., Coorssen, J.R., Shortland, P.J., 2022. The roles of microglia and astrocytes in phagocytosis and myelination: insights from the cuprizone model of multiple sclerosis. Glia 70, 1215–1250. https://doi.org/10.1002/GLIA.24148.

Skripuletz, T., Gudi, V., Hackstette, D., Stangel, M., 2011. De- and remyelination in the CNS white and grey matter induced by cuprizone: the old, the new, and the unexpected. Histol. Histopathol. 26, 1585–1597. https://doi.org/10.14670/HH-26.1585.

Skripuletz, T., Lindner, M., Kotsiari, A., Garde, N., Fokuhl, J., Linsmeier, F., Trebst, C., Stangel, M., 2008. Cortical demyelination is prominent in the murine cuprizone model and is strain-dependent. Am. J. Pathol. 172, 1053–1061. https://doi.org/10.2353/ajpath.2008.070850.

Stevens, B., Porta, S., Haak, L.L., Gallo, V., Fields, R.D., 2002. Adenosine: a neuron-glial transmitter promoting myelination in the CNS in response to action potentials. Neuron 36, 855–868. https://doi.org/10.1016/S0896-6273(02)01067-X.

Takeda, H., Tsuji, M., Matsumiya, T., 1998. Changes in head-dipping behavior in the hole-board test reflect the anxiogenic and/or anxiolytic state in mice. Eur. J. Pharmacol. 350, 21–29. https://doi.org/10.1016/s0014-2999(98)00223-4.

Tanaka, T., Murakami, K., Bando, Y., Yoshida, S., 2013. Minocycline reduces remyelination by suppressing ciliary neurotrophic factor expression after cuprizone-induced demyelination. J. Neurochem. 127, 259–270. https://doi.org/10.1111/JNC.12289.

Tanaka, Y., Kitabatake, K., Abe, R., Tsukimoto, M., 2020. Involvement of A2B receptor in DNA damage response and radiosensitizing effect of A2B receptor antagonists on mouse B16 Melanoma. Biol. Pharm. Bull. 43, 516–525. https://doi.org/10.1248/BPB.B19-00976.

Theparambil, S.M., Kopach, O., Braga, A., Nizari, S., Hosford, P.S., Sagi-Kiss, V., Hadjihambi, A., Konstantinou, C., Esteras, N., Gutierrez Del Arroyo, A., Ackland, G. L., Teschemacher, A.G., Dale, N., Eckle, T., Andrikopoulos, P., Rusakov, D.A., Kasparov, S., Gourine, A.V., 2024. Adenosine signalling to astrocytes coordinates brain metabolism and function. Nature 632, 139–146. https://doi.org/10.1038/S41586-024-07611-W.

Trincavelli, M.L., Tonazzini, I., Montali, M., Abbracchio, M.P., Martini, C., 2008. Short-term TNF-Alpha treatment induced A2B adenosine receptor desensitization in human astroglial cells. J. Cell. Biochem. 104, 150–161. https://doi.org/10.1002/jcb.21611.

Vega-Riquer, J.M., Mendez-Victoriano, G., Morales-Luckie, R.A., Gonzalez-Perez, O., 2019. Five decades of cuprizone, an updated model to replicate demyelinating diseases. Curr. Neuropharmacol. 17, 129–141. https://doi.org/10.2174/1570159X15666170717120343.

Wei, W., Du, C., Lv, J., Zhao, G., Li, Z., Wu, Z., Haskó, G., Xie, X., 2013. Blocking A2B adenosine receptor alleviates pathogenesis of experimental autoimmune encephalomyelitis via inhibition of IL-6 production and Th17 differentiation. J. Immunol. 190, 138–146. https://doi.org/10.4049/JIMMUNOL.1103721.

Ye, J.N., Chen, X.S., Su, L., Liu, Y.L., Cai, Q.Y., Zhan, X.L., Xu, Y., Zhao, S.F., Yao, Z.X., 2013. Progesterone alleviates neural behavioral deficits and demyelination with reduced degeneration of oligodendroglial cells in cuprizone-induced mice. PLoS One 8. https://doi.org/10.1371/JOURNAL.PONE.0054590.

Yuan, X., Chittajallu, R., Belachew, S., Anderson, S., McBain, C.J., Gallo, V., 2002. Expression of the green fluorescent protein in the oligodendrocyte lineage: a transgenic mouse for developmental and physiological studies. J. Neurosci. Res. 70, 529–545. https://doi.org/10.1002/JNR.10368.

Zeisel, A., Hochgerner, H., Lönnerberg, P., Johnsson, A., Memic, F., van der Zwan, J., Häring, M., Braun, E., Borm, L.E., La Manno, G., Codeluppi, S., Furlan, A., Lee, K., Skene, N., Harris, K.D., Hjerling-Leffler, J., Arenas, E., Ernfors, P., Marklund, U., Linnarsson, S., 2018. Molecular Architecture of the mouse nervous System. Cell 174, 999–1014.e22. https://doi.org/10.1016/j.cell.2018.06.021.

Zhang, N., Zhang, R., Loers, G., Liu, C., Jin, L., Petridis, A.K., Zheng, X., Wang, Z., Siebert, H.C., 2020. Cuprizone-Induced demyelination in mouse hippocampus is alleviated by ketogenic diet. J. Agric. Food Chem. 68, 11215–11228. https://doi.org/10.1021/ACS.JAFC.0C04604.

Zirngibl, M., Assinck, P., Sizov, A., Caprariello, A.V., Plemel, J.R., 2022. Oligodendrocyte death and myelin loss in the cuprizone model: an updated overview of the intrinsic and extrinsic causes of cuprizone demyelination. Mol. Neurodegener. 17. https://doi.org/10.1186/S13024-022-00538-8.

Zoupi, L., Markoullis, K., Kleopa, K.A., Karagogeos, D., 2013. Alterations of juxtaparanodal domains in two rodent models of CNS demyelination. Glia 61, 1236–1249. https://doi.org/10.1002/GLIA.22511.